PROCEEDINGS OF SPIE

SPIEDigitalLibrary.org/conference-proceedings-of-spie

CT scout z-resolution improvement with image restoration methods

Zheng, Yufeng, Cui, Xiaohui, Wachowiak, Mark, Elmaghraby, Adel

Yufeng Zheng, Xiaohui Cui, Mark P. Wachowiak, Adel S. Elmaghraby, "CT scout z-resolution improvement with image restoration methods," Proc. SPIE 5032, Medical Imaging 2003: Image Processing, (15 May 2003); doi: 10.1117/12.480308

SPIE.

Event: Medical Imaging 2003, 2003, San Diego, California, United States

CT scout *z*-resolution improvement with image restoration methods

Yufeng Zheng, Xiaohui Cui, Mark P. Wachowiak, and Adel S. Elmaghraby
Dept. of Computer Science and Engineering, University of Louisville, Louisville, Kentucky, USA

ABSTRACT

Currently, new applications demand utilizing CT scout images for diagnostic purposes. However, many CT scout images cannot be used diagnostically due to their poor resolution, particularly in the direction of table movement. Spatial resolution generally can be improved with image restoration techniques. Based on the principles of Wiener filtering and inverse filtering, this paper presents a modified Wiener filtering approach in the frequency domain. The concept of equivalent target point spread function is introduced, which makes the restoration process steerable. Consequently, balancing resolution improvement with noise suppression is facilitated. Experiments compare the image quality with traditional inverse filtering and Wiener filtering. The modified Wiener filtering method has been shown to restore the scout image with higher resolution and lower noise.

Keywords: CT scout, image restoration, inverse filtering, resolution improvement, Wiener filtering

1. INTRODUCTION

A CT scout image is obtained with a moving table and a stationary gantry. The current scout image generation process is designed for providing landmarks for CT scan ranges (like axial scans and helical scans), such as the GE Medical Systems LightSpeed^{TM} scanner. The only requirement for the scout is that object boundaries are clear. However, new applications, such as utilizing scout image to replace x-ray film for diagnostic purposes in urology applications, demand higher image quality. Other applications may use scout images for assisted diagnosis instead of x-ray film. Patients are not exposed to additional radiation, and no extra operations are required, because the scout scan is a standard and necessary operation in most CT scans. But in current scout imaging, the spatial resolution in the table translation direction (z) is always lower than that of the channel direction (x). For instance, the spatial resolution is 0.58mm in the x direction and 1.25mm in the z direction for LightSpeed^{TM} scanners. Therefore, the objective is to improve z-axis resolution to be close to that of the x-axis while minimizing noise.

Following z-resolution improvement, it is desirable to enhance the scout image details and contrast. In general, a scout image has a wide dynamic range that is usually due to the large difference in absorbing x-rays between bones and soft tissue. For example, a scout from human subject by LightSpeed^{TM} scanner has dynamic range of 1.38×10^5 intensities, which is displayed after preprocessing. A CT axial image is usually observed by changing the window width and location, actually changing the CT number and its display range[1], which results in many views of the same image. For a scout image, it is inconvenient to observe the image by changing the window width and location because the CT number is not applicable to these images, and because the whole image should be examined with one view. Thus, the scout image has such a wide range that many important details will be lost when directly mapped to 256 intensities. In other words, the question is how to display a wide dynamic image within 256 gray levels. A fusion enhancement algorithm (FEA) is under development to resolve this problem, and some primary results are demonstrated in Section 5. A full discussion of this enhancement algorithm will be presented in a subsequent paper.

In this paper, the z-resolution improvement will be discussed in detail. A general solution is to deconvolve the degraded image with the system point spread function (PSF). The PSF can be measured or computed for the specified system. The PSF in the z-axis for scout scanning is calculated as shown in Fig. 1. Deconvolution can be performed in the spatial or frequency domains. The frequency domain is preferred for convenient filter design and analysis. In this domain, inverse filtering and Wiener filtering are standard restoration methods for low-level noise systems such as CT scanners. However, with these methods, computations involving discrete quantities often lead to an ill-posed problem. Although regularization is very effective[2,3], in the case of CT scout imaging, the goal is to balance resolution improvement and noise suppression.

To improve the CT scout resolution in *z*-axis, a modified Wiener filtering (MWF) method was developed. The rest of the paper is organized as follows. In Section 2, the traditional Wiener filtering procedure is described. The MWF process is introduced in Section 3, where inverse filtering is also analyzed. Although the MWF is explained in frequency domain, there is a physical interpretation to MWF in spatial domain, as stated in this section. Experiments and results are given in Section 4 and 5. Section 6 concludes the paper.

2. WIENER FILTERING

A CT scanner can be modeled as a linear system that is also time and position invariant in the *z*-axis[4]. The scout sampling process in the *z*-direction is modeled as:

$$g(z) = f(z) * h(z) + n(z), \tag{1}$$

where $g(z)$ denotes the degraded scout data measured, $f(z)$ is the uncorrupted data, $h(z)$ is the system PSF in the z direction, the symbol * denotes convolution, and $n(z)$ is position-independent additive noise.

From convolution theory, Eq. (1) can be expressed in the frequency domain as:

$$G(u) = H(u)F(u) + N(u). \tag{2}$$

By considering signal and noise as random processes, the objective is to find an estimate $\hat{f}(z)$ of the uncorrupted signal $f(z)$ such that the mean square error between them is minimized[5]. This error measure is given by:

$$e^2 = \int_{-\infty}^{+\infty} \left| f(z) - \hat{f}(z) \right|^2 dz. \tag{3}$$

It is assumed that the signal and noise are uncorrelated, that the noise has zero mean, and that the gray levels in the estimate are linearly related to the levels in the degraded image. Based on these conditions, the minimum of the error function in Eq. (3) is given in the frequency domain by the expression[6]:

$$\hat{F}(u) = \left[\frac{H^*(u)}{\left| H(u) \right|^2 + S_n(u)/S_f(u)} \right] G(u), \tag{4}$$

where $H^*(u)$ denotes the complex conjugate of $H(u)$, $|H(u)|^2 = H^*(u)H(u)$, $S_n(u) = |N(u)|^2$ is the power spectrum of the noise, and $S_f(u) = |F(u)|^2$ is the power spectrum of the uncorrupted signal. The term in square brackets is known as the Wiener filter. When the noise is spectrally white, the spectrum $S_n(u)$ is constant. However, $S_f(u)$ is unknown. In general, a positive constant K is used to approximate $S_n(u)/S_f(u)$ in Eq. (4), which is simplified as:

$$\hat{F}(u) = \left[\frac{H^*(u)}{\left| H(u) \right|^2 + K} \right] G(u). \tag{5}$$

Wiener filtering can give good results in resolution improvement, but the restored image is frequently corrupted by the increased noise and aliasing, which is especially unacceptable for diagnostic medical images.

3. MODIFIED WIENER FILTERING

Assuming that the noise level is low enough to be temporally negligible, an estimate of the original signal can be computed from Eq. (2) as follows:

$$\hat{F}(u) = \left[\frac{1}{H(u)}\right] G(u). \tag{6}$$

This, in fact, is direct inverse filtering. It results in an ill-posed problem when $H(u)$ is zero or very small, as shown in Fig. 2. However, inverse filtering is equivalent to restoring the system PSF to an ideal delta function (referred to as target PSF) in the spatial domain. Experiments show that inverse filtering often leads to an over-corrected result. In other words, noise and aliasing are increased (as marked in Fig. 5), and the restored image appears to be noisier than the original.

Therefore, a Gaussian function, instead of a delta function, is used as the target PSF, t_{psf} (the equivalent PSF after performing image restoration), in the spatial domain. This PSF is shown in Fig. 1 (only the central part is illustrated here; actually this PSF should extend to the whole domain along z-axis), and is given as:

$$t_{psf}(z) = e^{-z^2/2\sigma^2}, \tag{7}$$

where σ is a positive real constant for adjusting the width of Gaussian span. Furthermore, $t_{psf}(z)$ tends to a delta function when σ becomes very small. The restoration process is therefore steerable, because the shape of target PSF determines the restored image quality. Of course, other functions can also be used as a target PSF.

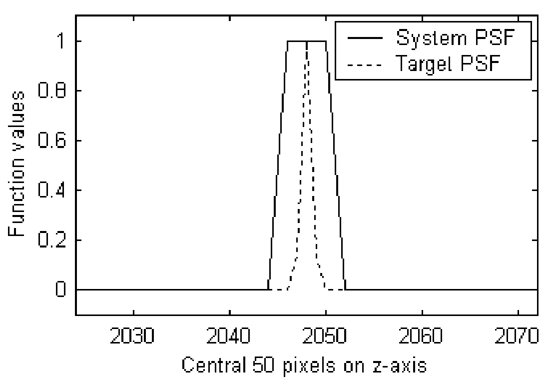

Figure 1: System PSF and Gaussian function (σ=0.5)

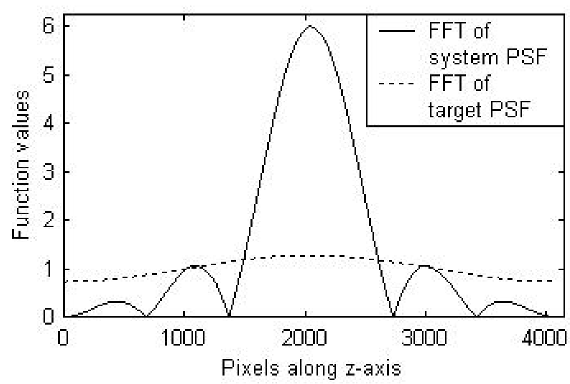

Figure 2: Fourier transform of PSFs in Fig. 1

Incorporating Eq. (7) into (6) yields:

$$\hat{F}(u) = \left[\frac{T_{psf}(u)}{H(u)}\right] G(u), \tag{8}$$

where $T_{psf}(u)$ (also a Gaussian function) is the Fourier transform of $t_{psf}(z)$. This is one reason why a Gaussian function is preferred as the target function. Better image quality can be achieved with Eq. (8) than with Eq. (6).

For the same reason, incorporating Eq. (7) into (5) yields:

$$\hat{F}(u) = \left[\frac{T_{psf}(u)H^*(u)}{|H(u)|^2 + K}\right] G(u), \tag{9}$$

where the term in square brackets is defined as the modified Wiener filter (MWF). In fact, MWF can be also considered as Gaussian low-pass filtering after Wiener filtering in frequency domain. From this standpoint, its effect on noise suppression can be explained.

4. EXPERIMENTS

Two CT scout images, a resolution phantom and a scan of a human subject (scanned with a GE LightSpeed™ system), are collected as the experimental data. Detector window and table movement causes the degradation of *z*-resolution during sampling. Consequently, the system PSF (Fig. 1) is considered as a convolution of two window functions (detector and sampling windows) that can be computed by system parameters such as detector size (in the *z*-axis), sampling frequency, and table translation speed. To observe image resolution clearly, a one-dimensional signal is resampled from the scout image along both the *x* and *z*-axes (as shown in Fig. 3). A difference image (subtraction of the processed image from the original) is used for observing noise level and aliasing. Filter normalization is necessary for constant signal energy before and after filtering.

The signal-to-noise ratio is a natural quantitative measure of image quality. However, the uncorrupted signal $f(z)$ is unknown, and the standard deviation is used to estimate the noise level. An $M \times N$-pixel region of interest (ROI) of homogeneous density is selected, as shown in Fig. 3. The standard deviation, σ_I, which is expected to be small, is computed.

5. RESULTS AND DISCUSSION

The original image is shown in Fig. 3, in which sampling lines and ROI (for standard deviation) are also displayed. The scout resolution in the *x*-axis can be clearly distinguished at level 4, as tagged on Fig. 4. As a comparison, inverse filtering results, with $\sigma = 1.0$ in Eq. (8) are also depicted in following figures. Although *z*-resolution could be effectively improved up to level 4 (Fig. 6), the restored image was evidently corrupted by enlarged noise and alias as shown in Fig.5. A quantitative measurement of noise level is σ_I(inverse) = 1.48, which is very large relative to σ_I(original) = 0.07.

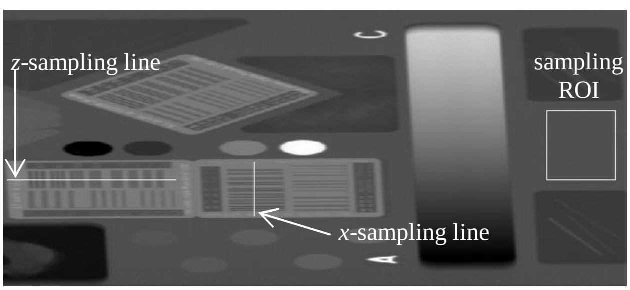

Figure 3: Original image with sampling line and ROI.

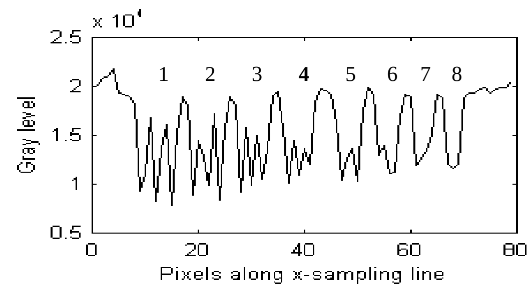

Figure 4: Resolution in *x*-axis.

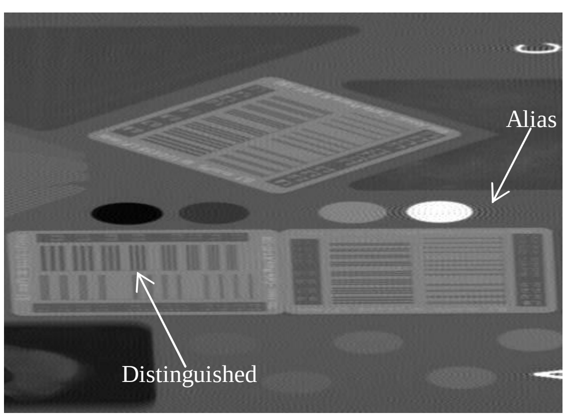

Figure 5: Restored image with inverse filtering.

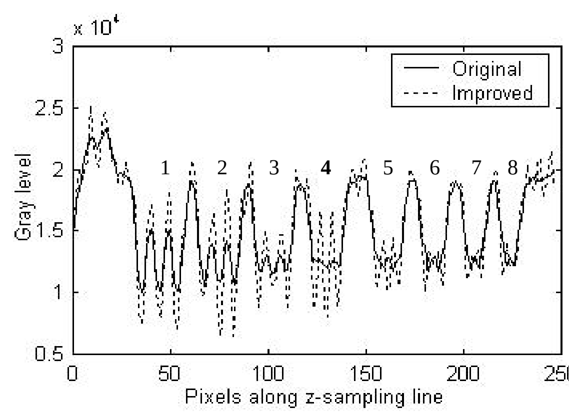

Figure 6: Resolution in *z*-axis with inverse filtering.

Figures 7, 9 and 11 are processed results corresponding to Wiener filtering with K = 0.8, and denote the restored image, difference image and z-resolution, respectively. Comparative results obtained by MWF filtering, with K = 0.8 and σ = 0.5, are displayed in Figs. 8, 10 and 12. The scout image dataset was over-sampled in z-axis so that the horizontal dimension is triple that of the vertical dimension. However, to observe z-resolution clearly, they are not down-sampled in the z-axis (except for Fig. 13), as they should with a 3:1 ratio for diagnostic purposes. The values of the K or σ parameters are selected interactively based on the restored image quality (IQ) of the experimental results. Clearly, with smaller K or σ, a higher the z-resolution will be obtained. On the other hand, however, small values of K or σ invariably result in increased noise and aliasing. It is pointless to restore the z-resolution to be higher than the x-resolution. Therefore, K and σ are chosen to be as large as possible, as long as the z-resolution attains level 5 (to guarantee a distinguished level 4 after down-sampling), as shown in Figs. 11 and 12.

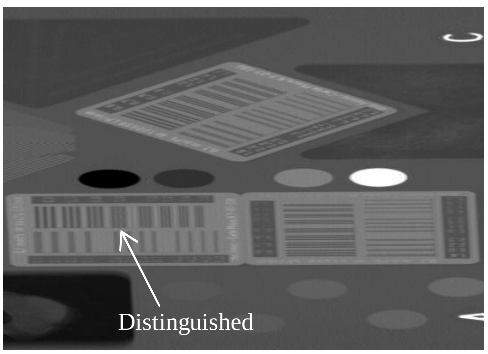

Figure 7: Restored image using Wiener filtering.

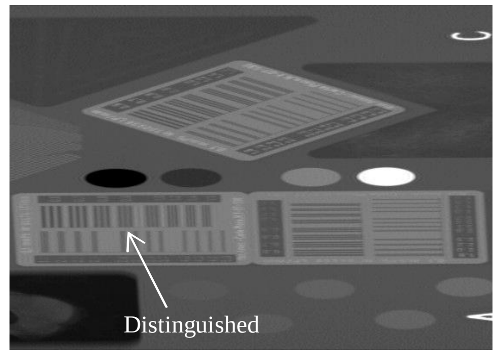

Figure 8: Restored image using MWF.

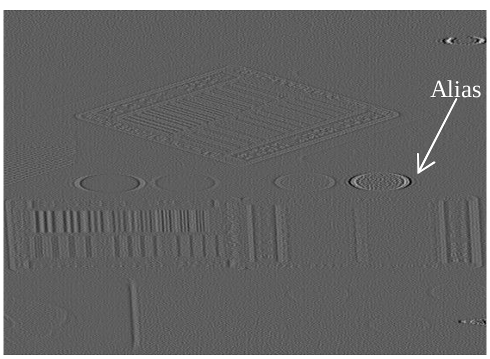

Figure 9: Difference image using Wiener filtering.

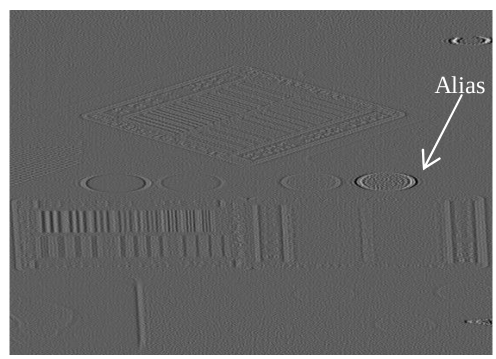

Figure 10: Difference image using MWF.

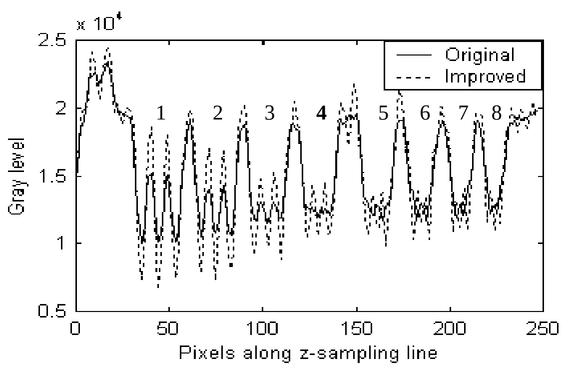

Figure 11: Resolution in z-axis using Wiener filtering.

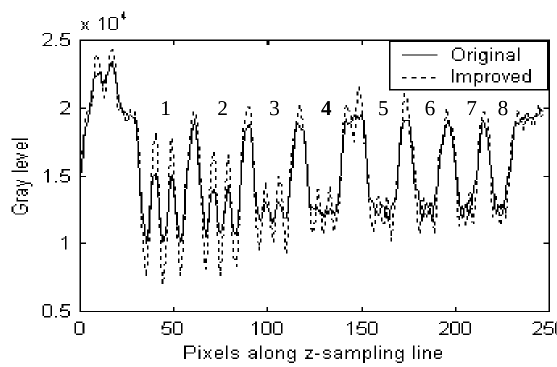

Figure 12: Resolution in z-axis using MWF.

Table 1: IQ variation with K for Wiener filtering

K	0.1	0.2	0.4	0.8	1.0
σ_I	0.97	0.68	0.44	0.27	0.22
Res.	8	7	6	5	4

Table 2: IQ variation with K for MWF ($\sigma = 0.5$)

K	0.1	0.2	0.4	0.8	1.0
σ_I	0.41	0.29	0.19	0.13	0.09
Res.	8	7	6	5	4

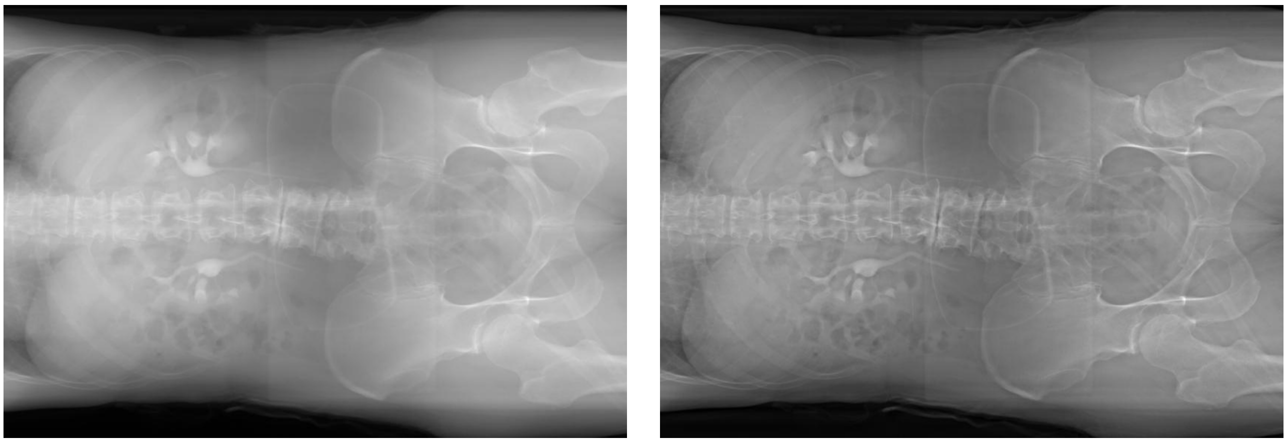

(a) Original image (b) Restored and enhanced image

Figure 13: Application of MWF followed by FEA to a human scan (already down-sampled in z-axis)

From the figures, it is difficult to judge which image has a higher IQ. Thus, noise level is examined. The standard deviation was computed as σ_I(original) = 0.07. In reality, the CT scout is a 16-bit dataset (Figs. 3, 8 and 9), but for comparative purposes, σ_I is calculated on the images scaled to the range [0, 255]. The standard deviation and z-resolution level (Res.) of the restored image, with varying K, are listed in Tables 1 and 2 for Wiener filtering and MWF, respectively. The restored IQ by MWF depends on both K and σ. However, only the IQs varying with K are presented. A suitable σ (= 0.5) is selected to easily determine a balance between resolution and noise. The Wiener filter with $K = 0.8$ resulted in σ_I(Wiener) = 0.27, about four times that of the original image. In contrast, by applying MWF filtering with $K = 0.8$ and $\sigma = 0.5$, only about twice the standard deviation of the original image was obtained (i.e. σ_I(MWF) = 0.13). It is evident that MWF restoration has a lower noise level than that of Wiener filtering.

The z-resolution improvement of applying MWF algorithm to a human scan is not as obvious as that of the phantom, because there are more overlapping details (small structures) in the human scout than in a phantom. So further processing is also required because of the reasons stated in the introduction. The FEA, still under development, presents an image fusion approach to preserve and enhance details of CT scout images. The enhanced image is obtained by high-boost filtering a smoothed image, which is computed by fusing a difference image and the original by applying an average rule. The difference image results from a fused image, which is calculated with a set of sub-images derived from the original. Image fusion is performed pixel-by-pixel with the discrete wavelet transform. Preliminary experimental results are demonstrated in Fig. 13. Image quality and noise level will be subsequently evaluated.

6. CONCLUSION

Experiments demonstrate that modified Wiener filtering can result in better restored image quality, judged on the basis of high image resolution and low level of noise and aliasing, achieved simultaneously. The concept of the steerable target PSF is introduced, which makes it possible to easily balance high resolution and low noise. This concept is suitable for general image restoration problems, although in the present paper, it is introduced specifically for improving CT scout image resolution. An enhancement algorithm is considered as a further postprocessing step.

7. REFERENCES

1. Gillespy, T, 3rd; Rowberg, A H; “Displaying radiologic images on personal computers: image processing and analysis”, *Journal of Digital Imaging*, Volume 7, Issue 2, pp. 51-60, May 1994.
2. E. Sekko, G. Thomas, et al., “A deconvolution technique using optimal Wiener filtering and regularization”, *Signal Processing*, vol. 72, pp. 23-32, 1999.
3. L. D'Amore, V. De Simone, and A. Murli, “The Wiener filter and Regularization methods for image restoration problems”, *Proc. of the 10th International Conference on Image Analysis and Processing*, September 1999.
4. Geoffrey Dougherty, “Effect of sub-pixel misregistration on the determination of the point spread function of a CT imaging system”, *Med. Eng. & Physics*, Vol. 22, pp. 503-507, Sep 2000.
5. William H. Press, Saul A. Teukolsky, et al., *Numerical Recipes in C* (Second Edition), Cambridge University Press, New York, NY, 1992.
6. Rafael C. Gonzalez, Richard E. Woods, *Digital Image Processing* (Second Edition), Prentice-Hall, Upper Saddle River, NJ, 2002.